AGU PUBLICATIONS

Geophysical Research Letters

RESEARCH LETTER
10.1002/2014GL059891

Key Points:
- We summarized paradoxes in research of SASM rainfall and circulation changes
- We raised and clarified one new paradox: Lower increases and upper reduces
- We analyzed contributions of moisture and lower/upper winds to rainfall change

Supporting Information:
- Readme
- Figure S1
- Figure S2

Correspondence to:
J. Ma,
tonyj.ma@gmail.com

Citation:
Ma, J., and J.-Y. Yu (2014), Paradox in South Asian summer monsoon circulation change: Lower tropospheric strengthening and upper tropospheric weakening, *Geophys. Res. Lett.*, *41*, 2934–2940, doi:10.1002/2014GL059891.

Received 11 MAR 2014
Accepted 31 MAR 2014
Accepted article online 2 APR 2014
Published online 16 APR 2014

Paradox in South Asian summer monsoon circulation change: Lower tropospheric strengthening and upper tropospheric weakening

Jian Ma[1] and Jin-Yi Yu[1]

[1]Department of Earth System Science, University of California, Irvine, California, USA

Abstract In the literature, there exist contradictory conclusions on the South Asian summer monsoon (SASM) precipitation and circulation changes: whether the circulation change contributes positively by strengthening or negatively by weakening to the rainfall enhancement, on a background of moisture content increase. Based on Representative Concentration Pathway 4.5 simulations by 18 Coupled Model Intercomparison Project phase 5 models, this study explains these puzzles by illustrating that the SASM circulation changes oppositely between the lower and upper troposphere, with tipping point at 450 hPa. However, this indicates a new paradox, created by competing mechanisms. By analyzing the intermodel variability, we determine that the mean advection of stratification change mechanism weakens the upper tropospheric circulation, while the enhanced surface land-sea thermal contrast strengthens the lower level and surface winds. Our moisture budget analysis shows that the SASM precipitation enhancement (8% K^{-1}) attributes to moisture increase (5% K^{-1}) and lower tropospheric circulation strengthening (3% K^{-1}).

1. Introduction

Constituting the most spectacular manifestation of the global climate system resulting from land-sea thermal contrast and orographic features, the South Asian summer monsoon (SASM) provides a major percentage (up to 80%) of annual precipitation over the world's most densely populated regions, e.g., India, and has tremendous impacts on agriculture, health, water resources, economies, and ecosystems throughout South Asia [*Webster et al*., 1998]. As an important part of the large-scale atmospheric circulation, its vigorous upward motion dominates the boreal summer Hadley circulation [*Trenberth et al*., 2005] with profound remote influences [*Zhang et al*., 2005].

A number of assessments on the response of the SASM to global warming have been attempted using projections from the World Climate Research Program's (WCRP's) Coupled Model Intercomparison Project (CMIP). While consistent evidences are found for the increase of the equilibrium SASM precipitation [*Douville et al*., 2000; *Ashrit et al*., 2005], contradictions stand among former studies on the monsoon circulation change in relation to the moisture and rainfall increase.

Despite a larger continental-scale land-sea thermal contrast in summer, the intensity of the monsoon circulation is predicted to reduce by 14% per century [*Tanaka et al*., 2005]. This weakening can be explained by the thermodynamic constraint discussed in *Held and Soden* [2006] or by the mean advection of stratification change (MASC) mechanism raised in *Ma et al*. [2012]. The principle of MASC is unique to global warming: on a background of global increase in static stability, the anomalous isotherms are apparently distorted by the advection of climatological vertical motion, which is equivalent to cooling/heating in the convective ascending/subsidence regions. Opposing the climatological thermal driving, this anomalous adiabatic forcing factor dynamically and effectively weakens any type of tropical tropospheric circulation, including the overturning and monsoon circulations. By definition, MASC is presumably an invariant independent of model or scenario but highly sensitive to the extent of the sea surface temperature SST warming. We confirm this property in the supporting information: in the SASM region, MASC forcing shows a high intermodel correlation coefficient (r) of −0.89 with the SST warming extent, in spite of differences in model physics (Figure S1).

The seemingly contradiction between the SASM rainfall increase and circulation reduction [*Kitoh et al*., 1997] can easily be interpreted as a result of the moisture increase from the warmer Indian Ocean and the consequent larger moisture transport/convergence over the monsoon region [*Ueda et al*., 2006; *Meehl and*

Table 1. The 18 WCRP's CMIP5 Models Adopted in This Study

Model Name	Modeling Center[a]	Country
ACCESS1.0	CSIRO-BOM	Australia
BCC-CSM1.1	BCC	China
CanESM2/AM4	CCCMA	Canada
CCSM4	NCAR	United States
CNRM-CM5	CNRM-CERFACS	France
GFDL-ESM2G	NOAA GFDL	United States
GISS-E2-R	NASA GISS	United States
HadGEM2-CC	MOHC	United Kingdom
HadGEM2-ES/-A	MOHC	United Kingdom
INM-CM4	INM	Russia
IPSL-CM5A-LR	IPSL	France
IPSL-CM5A-MR	IPSL	France
MIROC5	MIROC	Japan
MIROC-ESM-CHEM	MIROC	Japan
MIROC-ESM	MIROC	Japan
MPI-ESM-LR	MPI-M	Germany
MRI-CGCM3	MRI	Japan
NorESM1-M	NCC	Norway

[a]Modeling centers are as follows: CSIRO-BOM = Commonwealth Scientific and Industrial Research Organisation-Bureau of Meteorology, BCC = Beijing Climate Center, CCCMA = Canadian Centre for Climate Modelling and Analysis, NCAR = National Center for Atmospheric Research, CNRM-CERFACS = Centre National de Recherches Météorologiques-Centre Europeen de Recherche et de Formation Avancée en Calcul Scientifique, NOAA GFDL = National Oceanic and Atmospheric Administration Geophysical Fluid Dynamics Laboratory, NASA GISS = National Aeronautics and Space Administration Goddard Institute for Space Studies, MOHC = Met Office Hadley Centre, INM = Instituto Nacional de Meteorología, IPSL = Institut Pierre-Simon Laplace, MIROC = Model for Interdisciplinary Research on Climate, MPI-M = Max-Planck-Institut for Meteorology, MRI = Meteorological Research Institute, and NCC = Norwegian Climate Centre.

Arblaster, 2003; *May*, 2004]. However, the projected monsoon rainfall growth rate (up to ~8.4% K^{-1} [*Kripalani et al.*, 2007] or ~12.5% K^{-1} [*Annamalai et al.*, 2007]) is higher than that of column vapor (7% K^{-1} [*Held and Soden*, 2006]), which implies an increase in the monsoon circulation. Indeed, *Hu et al.* [2000] reported intensifications of both SASM precipitation and circulation due to the enhancement of the land-sea thermal gradient.

The present study aims to clarify the apparent contradictions of the SASM circulation change (strengthening or weakening) found in the literature. After an in-depth examination, we discovered that studies suggesting the monsoon circulation weakening tend to focus on the upper troposphere [e.g., *Tanaka et al.*, 2005; *Ueda et al.*, 2006], whereas monsoon wind strengthening are usually found in the lower troposphere near surface [*Hu et al.*, 2000]. Using the CMIP5 output, we look separately into changes of SASM surface and 200 hPa winds in relation to surface and air temperature changes. Mechanisms controlling the circulation change are investigated. Eventually, the vertical profile of SASM circulation change is illustrated, and a rainfall change budget is calculated, attributing to moisture content increase and lower/upper level circulation change according to the profile.

2. Data and Method

Representative Concentration Pathway (RCP) 4.5 simulations by 18 CMIP5 models (Table 1) are used in this study. These models provide various lengths of simulations with the future radiative forcing stabilized at 4.5 W m^{-2} in 2100 [*Thomson et al.*, 2011]. We analyze one realization (r1i1p1) for each model during the period 2006–2098. All results are averages during June-July-August (JJA). Changes are calculated as the difference between means of two 10 year periods: 2089–2098 minus 2006–2015. They are then normalized by the tropical (20°S–20°N) mean sea surface temperature (SST) warming in each model before calculating ensemble means, except for Figure 2 where warming extent are retained to realize the influences of land-sea thermal contrast change and average warming (MASC).

The SASM precipitation and circulation indices are defined based upon the multiple indices discussed in *Wang and Fan* [1999]. Our indices cover a larger area than the all-Indian summer rainfall and the Webster and Yang indices: 0–30°N, 70–110°E (the magenta square in Figure 1a). Since zonal wind is generally much stronger than meridional, it is used to calculate circulation indices at surface and upper level (Figure 2) and in combination with scalar wind speed for vertical profile (Figure 3).

We perform a moisture budget analysis (Figure 4) to decompose the atmospheric dynamic and thermodynamic contributions to rainfall change [*Seager et al.*, 2010]. Once the atmospheric moisture equation is vertically integrated, one obtains

$$\overline{P-E} = -\left\langle \nabla \cdot \left(\overline{\mathbf{V}} \cdot \overline{q} \right) \right\rangle + \text{Eddy}, \quad (1)$$

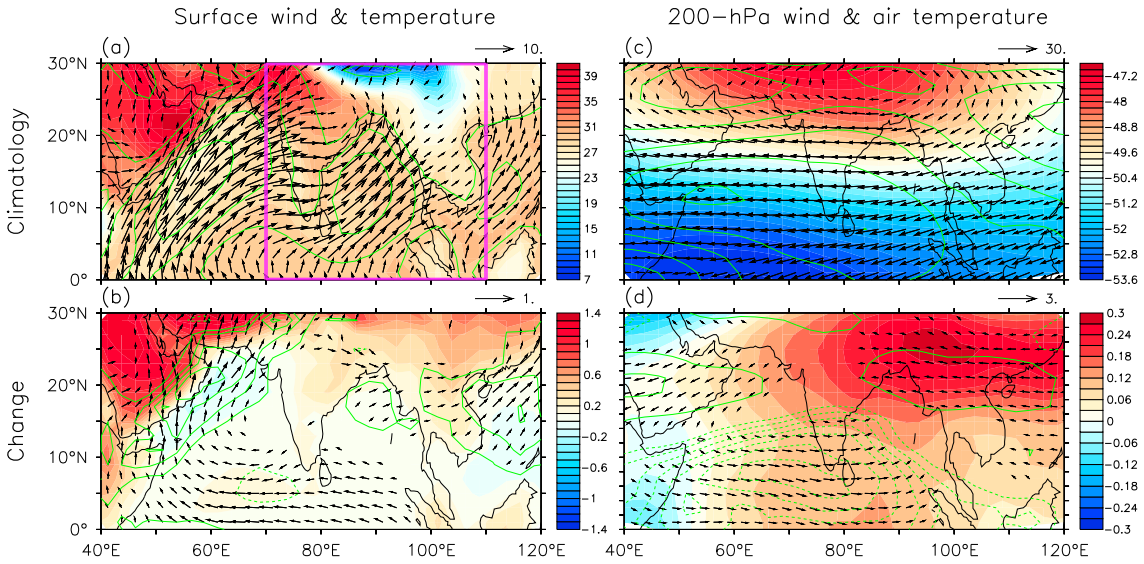

Figure 1. Ensemble and JJA mean (a and c) climatologies and (b and d) changes of (a and b) surface wind (vectors in m s^{-1}) and temperature (color shading in K) and (c and d) 200 hPa wind (vectors in m s^{-1}) and air temperature (color shading in K), simulated in the 18 CMIP5 models along RCP4.5. Contours show the wind speed climatology (Contour Interval; CI: 2.5 m s^{-1}) and change (CI: 0.1 m s^{-1}). All changes are scaled by the tropical (20°S–20°N) mean SST warming in each model. Surface temperature change here is deviations from the tropical mean SST warming, and air temperature change is deviations from the tropical mean air warming. The magenta square in Figure 1a marks the region (0°–30°N, 70°–110°E) in which the indices for zonal mean wind change are calculated.

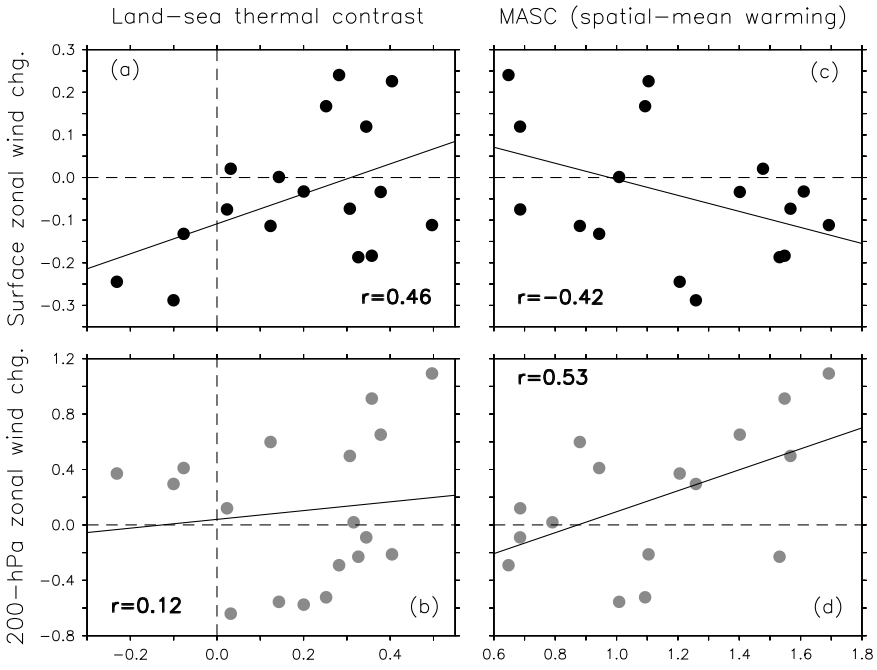

Figure 2. Relations between JJA mean changes in the (a and b) land-sea surface thermal contrast (K), (c and d) spatial mean surface warming (K), and zonal wind at surface (m s^{-1}) as shown in Figures 2a and 2c, upper level (m s^{-1}) as shown in Figures 2b and 2d, calculated in the region of 0°–30°N, 70°–110°E (magenta square in Figure 1a) among the 18 CMIP5 simulations along RCP4.5. The results here are not scaled to reserve the influence of warming extent.

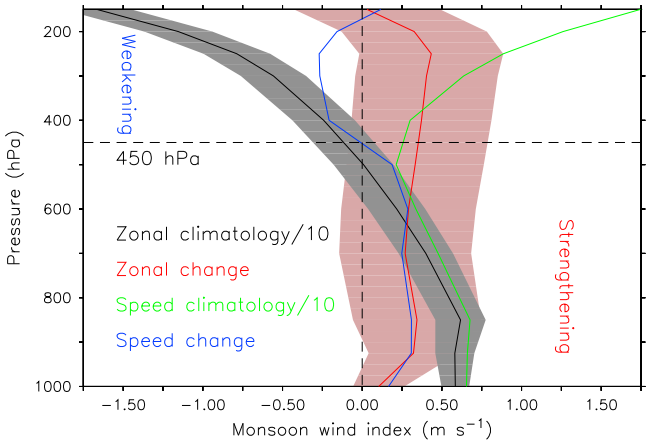

Figure 3. Ensemble and JJA mean vertical profiles of climatology (10 m s^{-1}) and change (m s^{-1}) of SASM zonal wind and wind speed indices (0°–30°N, 70°–110°E) in the RCP4.5 simulations of the 18 CMIP5 models. Shadings mark the uncertainty (±1 standard deviation) of the zonal wind.

where P is precipitation, E is evaporation, $< >$ represents column mass integration throughout the troposphere (approximated as 200–1000 hPa), and the overbar denotes the monthly average. $\mathbf{V}$ denotes atmospheric velocity. The eddy term is due to submonthly variability.

In global warming, the perturbation of $P - E$ can be linearly decomposed as

$$\delta\left(\overline{P-E}\right) \approx -\int_{200\text{hPa}}^{1000\text{hPa}} \left\langle \nabla \cdot \left(\overline{\mathbf{V}} \cdot \delta \overline{q}\right) \right\rangle - \int_{450\text{hPa}}^{1000\text{hPa}} \left\langle \nabla \cdot \left(\delta \overline{\mathbf{V}} \cdot \overline{q}\right) \right\rangle - \int_{200\text{hPa}}^{450\text{hPa}} \left\langle \nabla \cdot \left(\delta \overline{\mathbf{V}} \cdot \overline{q}\right) \right\rangle, \quad (2)$$

where the first term on the right-hand side represents the contribution of moisture content change and the second/third term lower/upper level circulation change.

3. Results

Surface wind is important for the SASM lower level moisture transfer/convergence and convection trigger, which is baroclinically in thermal wind balance with the upper level wind. In order to investigate the possibly

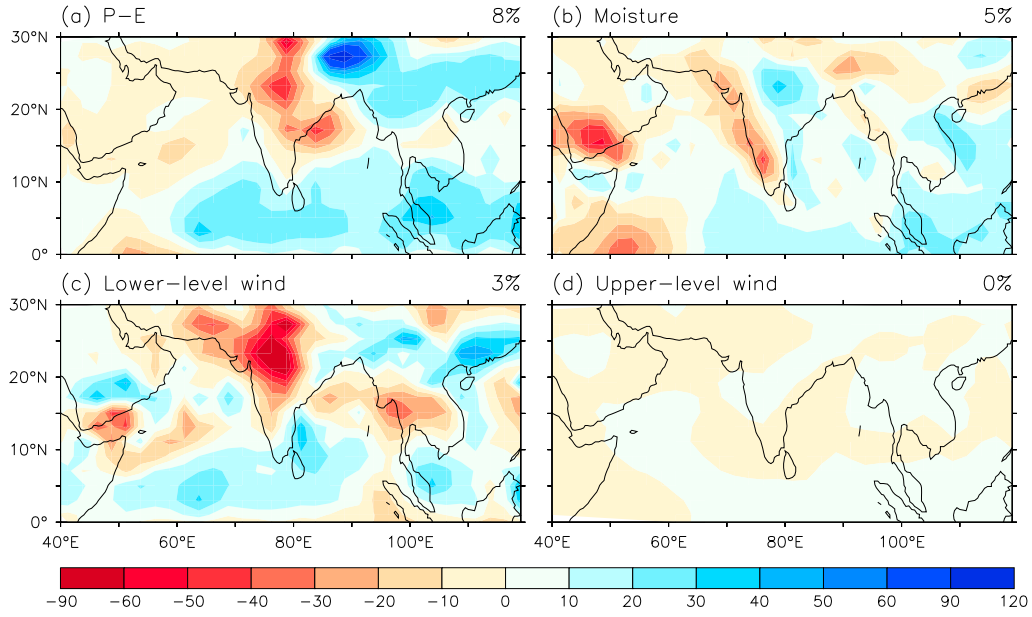

Figure 4. Ensemble and JJA mean moisture budget terms for change of precipitation minus evaporation (equation (2), mm $month^{-1}$) projected by the 18 CMIP5 models along RCP4.5.

paradoxical behaviors between lower and upper level SASM circulation changes, Figure 1 illustrates both the surface and upper level (200 hPa) wind velocity and speed changes in the ensemble mean of the 18 CMIP5 RCP4.5 simulations, with their climatologies for reference. In Figure 1a, strong climatological surface southwesterlies prevail from the Arabian Sea, through the Bay of Bengal, to the South China Sea, bringing abundant moisture from the North Indian Ocean to the Asian continent and triggers convections anchoring the windward slope of topography, apparently driven by the lower level land-sea thermal contrast. Change of the surface wind (Figure 1b) shows coherent features with the climatology, especially in the Arabian and South China Seas, with increased lower level SASM wind speed, consistent with enhanced land-sea thermal contrast. In contrast, a climatological anticyclone dominates the upper troposphere (Figure 1c) over the SASM region, centered at the Tibetan Plateau, due to the elevated heating there. Change of the 200 hPa wind (Figure 1d) is opposite to the climatology over the North Indian Ocean, with reduced upper level monsoon wind speed, associated with weak atmospheric warming there. This circulation reduction pattern is accordant with the MASC behavior for convective region. These results showing surface wind strengthening and upper level wind weakening confirm what we found in the literature to explain the contradictions in former studies.

However, Figure 1 apparently raises a new paradox between the SASM circulation changes in lower and upper troposphere, which cannot be explained by one single mechanism but probably by competing mechanisms behind the scene. From the literature, we learned that enhanced land-sea thermal contrast is possible to enhance the SASM circulation, while MASC tends to reduce any type of tropical circulation, including the SASM. In order to examine these mechanisms, we look into the intermodel relationship between the changes of zonal wind at surface/upper level and land-sea thermal contrast/MASC in the CMIP5 RCP4.5 simulations (Figure 2). The land-sea thermal contrast in Figures 2a and 2b are defined by the difference between the average warming of land and that of ocean in the SASM index region (0–30°N, 70–110°E; marked by the magenta square in Figure 1a). As mentioned in section 1 and illustrated in Figure S1, the MASC effect is much influenced by the SST warming extent, so the average SST warming in the SASM index region is used to represent MASC in Figures 2c and 2d.

Figure 2a shows a linear relation between the changes of land-sea thermal contrast and the surface zonal wind with an intermodel correlation (r) of 0.46, passing the 95% significance level, while a low correlation (0.12) is found at 200 hPa (Figure 2b), which indicates that although the land-sea thermal contrast plays a key role in strengthening the SASM lower level wind, its effect cannot reach far to the upper troposphere. In contrast, the MASC effect is found to weaken the SASM circulation throughout the column, with high correlations with both surfaces ($r = -0.42$; Figure 2c) and upper level ($r = 0.53$; Figure 2d) zonal wind changes, passing the 90% and 99% significance levels, respectively. A sample illustration of the MASC effect on surface and upper level SASM circulation is shown in Figure S2, with a comparison with the latent heating effect. Nevertheless, in the lower troposphere near surface, the MASC effect is apparently overwhelmed by the enhanced land-sea thermal contrast, resulting in strengthened circulation.

Figure 2 clarifies the paradox in the SASM circulation change by competing mechanisms: weakened upper tropospheric wind by the MASC effect, and strengthened lower tropospheric and surface wind by the enhanced surface land-sea thermal contrast. Figure 3 summarizes these effects by showing the vertical profiles of climatology and change of the SASM zonal wind and wind speed averaged in the index region and among the 18 CMIP5 RCP4.5 simulations. In fact, barotropically across all tropospheric levels, the zonal wind change appears to be westerly (consistent with Figure 1), with two peaks at 850 hPa and 250 hPa, indicating the maximum effects of land-sea contrast and MASC, respectively. The uncertainty range marked by ensemble mean ±1 standard deviation shows that the sign of the SASM circulation change profile is robust among the models. However, because of the baroclinic nature of the climatological SASM circulation, the anomalous westerly weakens the upper tropospheric easterly wind but strengthens the lower tropospheric westerly wind. As clearly shown by the wind speed change, the apparent paradox in the SASM circulation change is created, with the tipping point at 450 hPa.

The moisture budget analysis formulated by equation (2) decomposes the change in the SASM $\delta\left(\overline{P-E}\right)$ into contributions from moisture content increase and lower and upper level circulation changes separated by the 450 hPa tipping point (Figure 4). The total $\delta\left(\overline{P-E}\right)$ (Figure 4a) shows a "wet-get-wetter" pattern [*Held and Soden*, 2006], increasing in the North Indian Ocean (I), off the west coast of India (II), along the Himalaya ridge (III), and from the northeastern Bay of Bengal through southern China (IV). This change pattern is

resulted from moisture increase (Figure 4b) in Regions I and III and from lower level wind strengthening (Figure 4c) in Regions I, II, and IV. Unsurprisingly, upper level wind weakening (Figure 4d) has little contribution due to lacking of moisture. Dominating $\delta(\overline{P-E})$, the percentage increase of the spatial mean rainfall in the SASM index region by 8% K^{-1} attributes to the moisture content increase by 5% K^{-1} and the lower tropospheric circulation enhancement by 3% K^{-1}, along with the tropical mean SST warming.

4. Conclusions

The present study has summarized four contradictions with explanations on the SASM precipitation and circulation changes in the literature:

1. Despite an enhancement in continental-scale surface land-sea thermal contrast in summer, the intensity of the monsoon circulation is predicted to reduce: Circulation weakened by the MASC mechanism;
2. Rainfall increases while circulation reduces: Precipitation enhancement is due to increase in water vapor content;
3. Rainfall growth rate is higher than that of column water vapor: Implication for circulation increase;
4. Circulation strengthening was reported, consistent with enhanced land-sea thermal contrast but inconsistent with other former research: Circulation weakening occurs in the upper troposphere, while strengthening occurs in the lower troposphere and near surface. More importantly, we have raised and clarified one new paradox with a related question:
5. Why is the circulation change opposite between the lower and upper troposphere? And how would this affect precipitation?

Confirming our findings in the literature, we have clearly shown that in global warming projections with the 18 CMIP5 models along RCP4.5, the SASM circulation change has a paradox: Wind increases at surface but deceases at upper level. Based on an intermodel variability analysis on possible mechanisms, we found that competing mechanisms are responsible for this paradox: The MASC effect weakens the upper tropospheric circulation, while the enhanced surface land-sea thermal contrast dominates the strengthening of the lower tropospheric and surface winds, though MASC tends to have a minor negative contribution.

The vertical profile of average zonal wind change in the SASM region shows a barotropic westerly consistent through all tropospheric levels. However, this barotropic westerly change has level-dependent meanings for the baroclinic climatology, strengthening the lower tropospheric westerly and weakening the upper tropospheric easterly, with tipping point at 450 hPa, as shown by the wind speed change profile. Our moisture budget analysis unsurprisingly suggests no significant contribution of the upper level circulation reduction to the SASM rainfall change due to low moisture content, and the precipitation change pattern attributes to both moisture content increase and lower level wind enhancement, which contribute 5% K^{-1} and 3% K^{-1}, respectively, to the total spatial mean precipitation increase of 8% K^{-1}, along with the tropical mean SST increase.

Acknowledgments

We acknowledge various modeling groups for producing and providing their output, the PCMDI for collecting and archiving the CMIP5 multimodel data set, the WCRP's WGCM for organizing the analysis activity, and the Office of Science, U.S. Department of Energy for supporting this data set in partnership with the Global Organization for Earth System Science Portals. We thank S.-P. Xie, Y. Kosaka, and S.-I. An for helpful discussions. Two anonymous reviewers are appreciated for their constructive comments and suggestions. The Ferret program was used for analysis and graphics. This work is supported by NSF (AGS-1233542) and NOAA (NA11OAR4310102).

The Editor thanks two anonymous reviewers for their assistance in evaluating this paper.

References

Annamalai, H., K. Hamilton, and K. R. Sperber (2007), The South Asian summer monsoon and its relationship with ENSO in the IPCC AR4 simulations, *J. Clim.*, *20*, 1071–1092.

Ashrit, R. G., A. Kitoh, and S. Yukimoto (2005), Transient response of ENSO-monsoon teleconnection in MRI.CGCM2 climate change simulations, *J. Meteorol. Soc. Jpn.*, *83*, 273–291.

Douville, H., J.-F. Royer, J. Polcher, P. Cox, N. Gedney, D. B. Stephenson, and P. J. Valdes (2000), Impact of CO_2 doubling on the Asian summer monsoon: Robust versus model-dependent responses, *J. Meteorol. Soc. Jpn.*, *78*, 421–439.

Held, I. M., and B. J. Soden (2006), Robust responses of the hydrological cycle to global warming, *J. Clim.*, *19*, 5686–5699.

Hu, Z.-Z., M. Latif, E. Roeckner, and L. Bengtsson (2000), Intensified Asian summer monsoon and its variability in a coupled model forced by increasing greenhouse gas concentrations, *Geophys. Res. Lett.*, *27*, 2681–2684, doi:10.1029/2000GL011550.

Kitoh, A., S. Yukimoto, A. Noda, and T. Motoi (1997), Simulated changes in the Asian summer monsoon at times of increased atmospheric CO_2, *J. Meteorol. Soc. Jpn.*, *75*, 1019–1031.

Kripalani, R. H., J. H. Oh, A. Kulkarni, S. S. Sabade, and H. S. Chaudhari (2007), South Asian summer monsoon precipitation variability: Coupled climate model simulations and projections under IPCC AR4, *Theor. Appl. Climatol.*, *90*, 133–159, doi:10.1007/s00704-006-0282-0.

Ma, J., S.-P. Xie, and Y. Kosaka (2012), Mechanisms for tropical tropospheric circulation change in response to global warming, *J. Clim.*, *25*, 2979–994.

May, W. (2004), Potential future changes on the Indian summer monsoon due to greenhouse warming: Analysis of mechanisms in a global time slice experiment, *Clim. Dyn.*, *22*, 389–414.

Meehl, G. A., and J. M. Arblaster (2003), Mechanisms for projected future changes in South Asian monsoon precipitation, *Clim. Dyn.*, *21*, 659–675.

Seager, R., N. Naik, and G. A. Vecchi (2010), Thermodynamic and dynamic mechanisms for large-scale changes in the hydrological cycle in response to global warming, *J. Clim.*, *23*, 4651–4668.

Tanaka, H. L., N. Ishizaki, and D. Nohara (2005), Intercomparison of the intensities and trends of Hadley, Walker and monsoon circulations in the global warming projections, *Sci. Online Lett. Atmos.*, *1*, 77–80, doi:10.2151/sola.2005-021.

Thomson, A. M., et al. (2011), RCP4.5: A pathway for stabilization of radiative forcing by 2100, *Clim. Change*, *109*, 77–94, doi:10.1007/s10584-011-0151-4.

Trenberth, K. E., J. W. Hurrell, and D. P. Stepaniak (2005), The Asian monsoon: Global perspectives, in *Asian Monsoon*, edited by B. Wang, pp. 67–87 (and color section 9-19), Springer/Praxis Publishing Ltd., New York.

Ueda, H., A. Iwai, K. Kuwako, and M. E. Hori (2006), Impact of anthropogenic forcing on the Asian summer monsoon as simulated by eight GCMs, *Geophys. Res. Lett.*, *33*, L06703, doi:10.1029/2005GL025336.

Wang, B., and Z. Fan (1999), Choice of South Asian summer monsoon indices, *Bull. Am. Meteorol. Soc.*, *80*, 629–638, doi:10.1175/1520-0477(1999)080<0629:COSASM>2.0.CO;2.

Webster, P. J., V. O. Magaña, T. N. Palmer, J. Shukla, R. A. Tomas, M. Yanai, and T. Yasunari (1998), Monsoons: Processes, predictability, and the prospects for prediction, *J. Geophys. Res.*, *103*(C7), 14,451–14,510, doi:10.1029/97JC02719.

Zhang, P., S. Yang, and V. E. Kousky (2005), South Asian high and Asian-Pacific-American climate teleconnection, *Adv. Atmos. Sci.*, *22*, 915–923, doi:10.1007/BF02918690.